JOURNAL OF BACTERIOLOGY, Dec. 2004, p. 8221–8228 Vol. 186, No. 24
0021-9193/04/$08.00+0 DOI: 10.1128/JB.186.24.8221–8228.2004

HMW1 Is Required for Stability and Localization of HMW2 to the Attachment Organelle of *Mycoplasma pneumoniae*

Melisa J. Willby,† Mitchell F. Balish,‡ Stephanie M. Ross, Kyungok K. Lee, Jarrat L. Jordan, and Duncan C. Krause*

Department of Microbiology, University of Georgia, Athens, Georgia

Received 29 June 2004/Accepted 15 September 2004

The cytoskeletal proteins HMW1 and HMW2 are components of the terminal organelle of the cell wall-less bacterium *Mycoplasma pneumoniae*. HMW1 is required for a tapered, filamentous morphology but exhibits accelerated turnover in the absence of HMW2. Here, we report that a reciprocal dependency exists between HMW1 and HMW2, with HMW2 subject to accelerated turnover with the loss of HMW1. Furthermore, the instability of HMW2 correlated with its failure to localize to the attachment organelle. The C-terminal domain of HMW1 is essential for both function and its accelerated turnover in the absence of HMW2. We constructed HMW1 deletion derivatives lacking portions of this domain and examined each for stability and function. The C-terminal 41 residues were particularly important for proper localization and function in cell morphology and P1 localization, but the entire C-terminal domain was required to stabilize HMW2. The significance of these findings in the context of attachment organelle assembly is considered.

The cell wall-less prokaryote *Mycoplasma pneumoniae* causes tracheobronchitis and primary atypical pneumonia in humans. Mycoplasma adherence to host respiratory epithelium (cytadherence) is mediated largely by the attachment organelle, a polar, membrane-bound, differentiated cell extension that is defined by an electron-dense core (7, 15). Extraction of *M. pneumoniae* cells with the nonionic detergent Triton X-100 (TX) yields a TX-insoluble fraction that includes this core structure and consists largely of cytoskeletal proteins such as HMW1, HMW2, HMW3, and P65 (Table 1) (6, 11, 13, 20, 30, 36). These proteins contribute to the architecture of the attachment organelle, including the localization of the major adhesin protein P1 to this structure, but little is known regarding their specific roles or the dynamics of their assembly (19).

HMW1 is a peripheral membrane protein on the mycoplasma cell surface but lacks typical secretion signal or transmembrane sequences or significant homology to any proteins found beyond the mycoplasmas (2, 3, 9). HMW1 has been localized to the attachment organelle (30, 32) as well as the trailing filament (32), depending upon the experimental approach. Cytadherence mutant M6 (Table 1) lacks HMW1 and produces the truncated cytadherence-associated protein P30 due to an internal, in-frame deletion (22). This mutant has a striking morphology, lacking the tapered filamentous appearance characteristic of wild-type cells, and fails to localize P1 to the attachment organelle (13). Recombinant wild-type HMW1, but not a truncated derivative lacking the C-terminal 112 amino acids, restores a near-normal morphology and P1 clustering to mutant M6 (13), indicating that HMW1 contributes to the architecture of the attachment organelle and that the C-terminal domain of HMW1 is essential for normal function.

HMW2 is a large protein predicted to form dimeric coiled coils, as well as trimeric coiled coils with P28, also a product of the *hmw2* gene (5, 21). HMW2 is a component of the attachment organelle and appears to be essential for assembly of the electron-dense core (5), which is absent in the *hmw2* mutant I-2 (20, 31). Loss of HMW2 also results in failure to localize the adhesin proteins P1 and P30 normally to the attachment organelle (6, 31), reduced cytadherence (20), altered cell morphology (6), and decreased steady-state levels of HMW1, HMW3, P65, and P30 (Table 1) (3, 17, 26). Wild-type recombinant HMW2 restores a normal phenotype to mutant I-2 (10), and a recombinant HMW2 internal-deletion derivative lacking approximately 80% of the protein (HMW2 Δmid) restores normal cell morphology and stability of HMW3 and P65 in mutant I-2 transformants (4). However, HMW2 Δmid fails to restore HMW1 stability or proper localization of P1 to the attachment organelle (4), reinforcing the functional association between HMW1 and P1 (13).

In the present study, we report that the stability of HMW2 is likewise dependent upon HMW1. A fourfold decrease in steady-state HMW2 was observed in mutant M6 relative to

TABLE 1. Protein profiles of wild-type and cytadherence mutant *M. pneumoniae*

M. pneumoniae	Protein[a]						Reference
	HMW1	HMW2	HMW3	P30	P30 Δ[b]	P65	
Wild type	++++	++++	++++	++++	−	++++	20, 23
Mutant I-2	+	−	++	+++	−	++	20
Mutant M6	−	+	++	−	++	+	17, 22
Mutant II-7	++++	++++	++++	−	++	+	8, 17, 20

[a] Symbols indicate relative amounts of each protein ranging from − (none) to ++++ (wild type).
[b] Mutants M6 and II-7 have an internal, in-frame deletion in the gene encoding P30, resulting in an identical truncated P30, designated P30 Δ.

* Corresponding author. Mailing address: Department of Microbiology, 523 Biological Sciences Bldg., University of Georgia, Athens, GA 30602. Phone: (706) 542-2671. Fax: (706) 542-2674. E-mail: dkrause@uga.edu.
† Present address: Department of Microbiology and Immunology, Emory University, Atlanta, Ga.
‡ Present address: Department of Microbiology, Miami University, Oxford, Ohio.

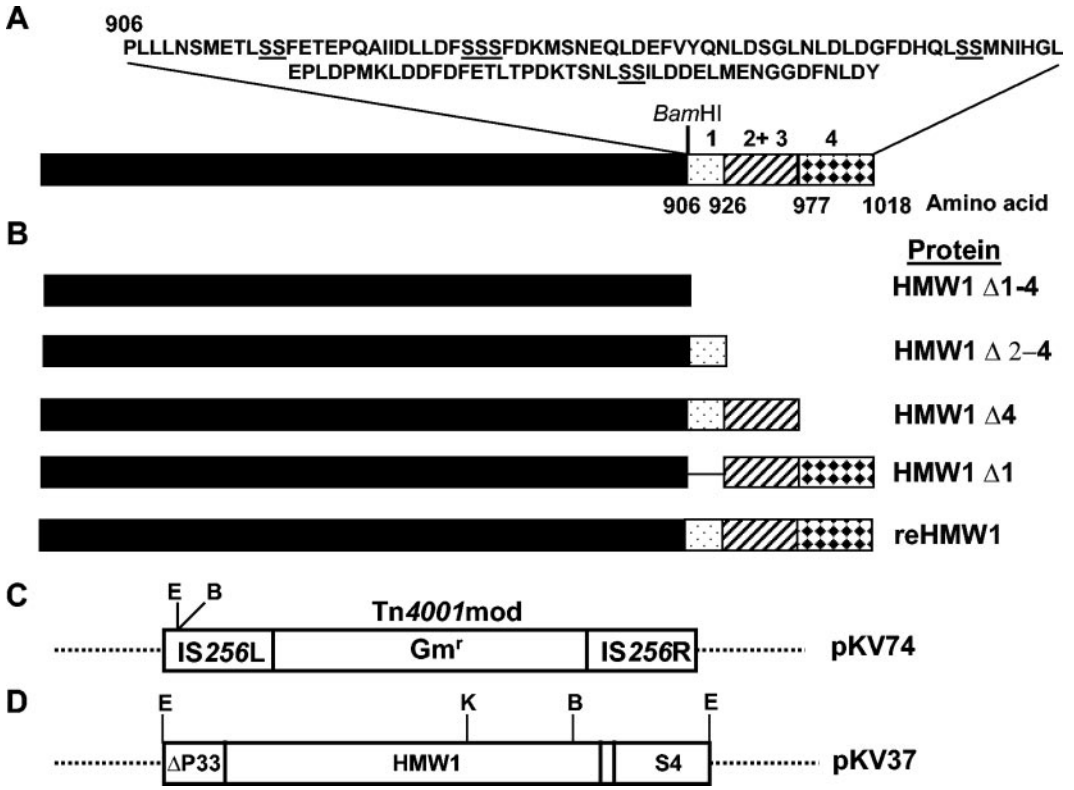

FIG. 1. Schematic representation of HMW1 and recombinant HMW1 constructs. (A) HMW1 with the sequence of the C-terminal 112 amino acids shown above and paired Ser residues underlined. Regions affected by deletion are represented by patterned boxes. The numbers above each correspond to the four paired Ser residues. Amino acid positions corresponding to each region are indicated below the diagram, and the relative position of the BamHI site is shown for reference (not to scale). (B) HMW1 deletion derivatives, with protein designation indicated to the right for each. (C and D) Schematic of relevant regions of plasmids pKV74 and pKV37 (not to scale). Restriction sites: E, EcoRI; B, BamHI; K, KpnI; Gm^r, gentamicin resistance gene.

wild-type *M. pneumoniae*, the result of accelerated turnover. HMW2 instability in mutant M6 correlated specifically with loss of HMW1, the failure of HMW2 to localize to the attachment organelle, and the absence of an electron-dense core. Recombinant full-length HMW1 restored HMW2 stability and localization, but HMW1 truncated at the C terminus by 112 amino acids did not. Analysis of HMW1 deletion derivatives established more precisely that the C-terminal 41 residues of HMW1 were particularly important for normal function in the development of the attachment organelle.

MATERIALS AND METHODS

Strains and culture conditions. Wild-type *M. pneumoniae* strain M129-B18 (23) and cytadherence mutants I-2, II-7, and M6 (Table 1) (8, 20, 22) were cultured in Hayflick or SP-4 medium or on PPLO agar plates at 37°C (12, 35); gentamicin (18 μg/ml) was included for culture of transformants. Individual colonies were identified on PPLO agar plates by hemolytic plaque formation (12). *Escherichia coli* cells were cultured at 37°C in Luria-Bertani broth or on Luria-Bertani agar plates; 100 μg of ampicillin/ml was included for plasmid selection (28). Plasmids were isolated with the QIAprep Spin Miniprep kit (QIAGEN, Valencia, Calif.) and the QIAGEN Plasmid Maxi kit or by alkaline lysis (28). Plasmid pKV210 (5) contains within a modified Tn*4001* the wild-type *hmw2* gene preceded by the promoter for the *p65* gene (20), with the *gfp* gene cloned at a position that yields a sandwich fusion between amino acids 97 and 98 of HMW2 (5).

Western immunoblotting and TX fractionation. Steady-state levels of HMW2, resident and recombinant HMW1, and P1 were evaluated by sodium dodecyl sulfate-polyacrylamide gel electrophoresis (SDS-PAGE) with 3 and 4.5% polyacrylamide stacking and separating gels, respectively, and Western immunoblotting (12) with HMW1-specific serum (32) at a 1:10,000 dilution, P1-specific serum (6) at a 1:1,000 dilution, or HMW2-specific serum (reference 21 and this study) at a 1:1,000 dilution. Antiserum to HMW2 was prepared as described previously (32) against a peptide corresponding to amino acid residues 1 to 18 conjugated to keyhole limpet hemocyanin.

Pulse-chase analysis. The stability of newly synthesized HMW2 and HMW1 derivatives was assessed as previously described (26) with modifications. Briefly, mid-log-phase cultures (each, 25 ml) were harvested, and the resulting pellets were suspended in 5 ml of Dulbecco's modified Eagle's medium supplemented with 10% dialyzed fetal bovine serum and all amino acids except Met. Samples were incubated for 30 min at 37°C with [^{35}S]Met at 67 μCi/ml (>1,000 Ci/mmol; 1 Ci = 37 GBq; Amersham, Piscataway, N.J.), washed with 5 ml of Dulbecco's modified Eagle's medium-fetal bovine serum containing 1 mM Met at 4°C, suspended in 3 ml of fresh Hayflick or SP-4 medium by passage through a 25-gauge needle, and dispensed in 1-ml aliquots. After incubation at 37°C for the indicated times, cell suspensions were centrifuged, washed three times with cold 10 mM phosphate-buffered saline (PBS; pH 7.2), and analyzed by SDS-PAGE and autoradiography. HMW2 loss was quantitated from autoradiograms with Scion Image (Scion Corp., Frederick, Md.). Relative amounts were determined as previously described (2), using a 150-kDa protein observed to be stable as a reference.

Construction of HMW1 deletion derivatives. We engineered HMW1 deletion derivatives for functional analysis based upon the distribution of a paired Ser motif previously implicated in proteolytic turnover (26) and repeated four times within the C-terminal domain of HMW1 (Fig. 1A). Plasmid pKV37 (Fig. 1D) (9) was digested with EcoRI and BamHI to release a 3,496-bp fragment containing all but the last 112 amino acids of HMW1. This fragment was cloned into the corresponding sites within the modified Tn*4001* (Tn*4001*mod) in pKV74 (13) to create pKV202 (HMW1 Δ1-4). Portions of the 3′ end of the *hmw1* gene were amplified by PCR (Table 2) with pKV37 as template DNA, digested with BamHI, and ligated into BamHI-digested pKV202 to generate HMW1 Δ4 (Fig.

TABLE 2. PCR primers used for construction of HMW1 deletion derivatives

Plasmid	HMW1 derivative	Upstream primer[a]	Downstream primer[a]	Nucleotides amplified[b]
pKV205	HMW1 Δ4	GGATGGCGAAGCTAGACAG	AT**G**G**ATC**C**T**TATGGCTCTAAC	2666–2942
pKV219	HMW1 Δ1	TGA**G**GATC**C**CTTGGACTTCTCC	GGCG**G**GATC**C**TTTGAAATACTACC	2778–3116
pKV213	reHMW1	GGATGGCGAAGCTAGACAG	GGCG**G**GATC**C**TTTGAAATACTACC	2666–3116

[a] Altered nucleotides are shown in boldface.
[b] Numbers indicate position within the *hmw1* coding sequence (9).

1B). Downstream PCR primers introduced a BamHI restriction site and an in-frame stop codon, while the upstream primer used to generate HMW1 Δ1 introduced a BamHI site (Table 2). Wild-type and mutant M6 *M. pneumoniae* cells were transformed with plasmid DNA containing the recombinant transposons as previously described (14); transposon delivery was required because allelic exchange has not been reported for *M. pneumoniae*.

Phase-contrast and fluorescence microscopy. Mycoplasmas were prepared for phase-contrast–fluorescence microscopy for visualization of green fluorescent protein (GFP) as detailed previously (5). For analysis by phase-contrast–immunofluorescence, mycoplasmas cultured 12 to 48 h in Hayflick or SP-4 medium containing gentamicin but lacking phenol red to minimize background fluorescence were washed with PBS and fixed in 0.2% glutaraldehyde–2% formaldehyde in PBS for 1 h at room temperature. Coverslips were washed two times in PBS–0.05% Tween 20 for 5 min each, and cells were permeabilized in 0.1% TX for 20 s, followed by two washes (5 min each) in PBS–0.05% Tween 20. Coverslips were blocked in PBS with 3% bovine serum albumin–0.05% Tween 20 in a humid chamber overnight at 4°C, then inverted onto 100-μl drops of blocking solution with HMW2-specific antibodies, affinity purified as previously described (33), diluted 1:20, and incubated 1 h at room temperature. Alternatively, coverslips were blocked with PBS–5% nonfat dry milk–0.05% Tween 20 and probed with P1-specific monoclonal antibody or anti-HMW1 serum diluted in PBS–2% nonfat dry milk–0.05% Tween 20. Coverslips were washed and probed with Cy3-conjugated AffiniPure donkey anti-mouse or anti-rabbit immunoglobulin G (Jackson Immunologicals, West Grove, Pa.), diluted 1:100 or 1:75, respectively. Coverslips were then washed well and examined by phase-contrast–fluorescence microscopy with a Leica DM IRB inverted fluorescence microscope equipped with a 1.4 numerical aperture, 100× objective (Leitz Wetzlar, Wetzlar, Germany) and fluorescein isothiocyanate and Cy3 filter cube sets (Leica) as previously described (5). Images were captured with an ORCA-ER charge-coupled device camera (Hamamatsu Corp., Bridgewater, N.J.) and digitized with OpenLab imaging software (version 3.1.2, Lexington, Mass.). Digitized images were superimposed and false colorized with Adobe Photoshop, version 6.0 or 7.0 (San Jose, Calif.).

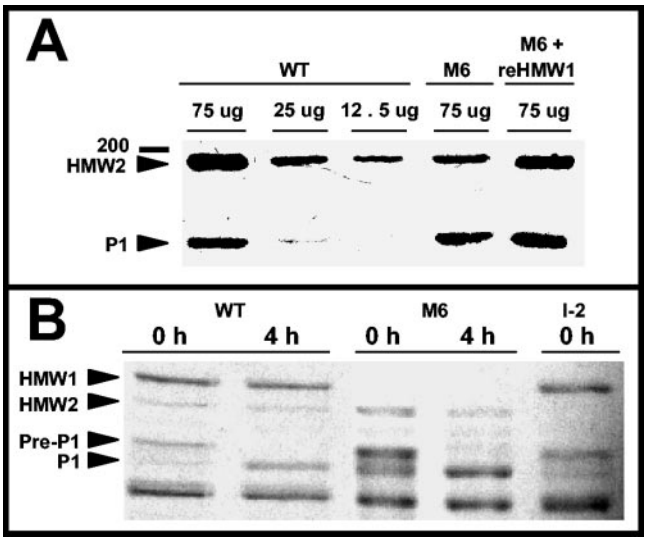

FIG. 2. (A) Western immunoblot analysis of HMW2 and P1 steady-state levels in wild-type and mutant M6 *M. pneumoniae*. Mycoplasma samples at the indicated protein concentrations were subjected to SDS-PAGE and Western immunoblotting with anti-HMW2 serum (1:1,000) and anti-P1 serum (1:1,000). Lanes: WT, 75, 25 or 12.5 μg of wild-type *M. pneumoniae* protein, as indicated; M6, 75 μg of protein from mutant M6; M6 + reHMW1, 75 μg of M6 transformant producing full-length recombinant HMW1. Arrowheads indicate HMW2 and P1, while the 200-kDa protein mass marker is shown to the left. (B) Pulse-chase analysis of HMW2 synthesis and turnover in wild-type (WT), mutant M6, and mutant I-2 *M. pneumoniae*. The arrowheads indicate HMW1, HMW2, pre-P1, and mature P1; time points are given at the top in hours.

RESULTS

HMW1 is required for HMW2 stability. Analysis by Western immunoblotting revealed an approximately fourfold decrease in steady-state HMW2 in mutant M6 relative to wild-type *M. pneumoniae*, while protein P1 levels, examined as an internal control, were indistinguishable (Fig. 2A). Pulse-chase studies demonstrated that HMW2 was subject to accelerated turnover in mutant M6 (Fig. 2B), where after 4 h newly synthesized HMW2 was reduced to 73.4% ± 8.9% of that at 0 h (mean and standard deviation from three experiments) and no reduction was evident in wild-type *M. pneumoniae*. We also observed wild-type levels of HMW2 in mutant II-7 but not in M6 expressing a recombinant wild-type *p30* allele (Table 1 and data not shown); thus, HMW2 instability correlated specifically with absence of HMW1 rather than truncation of P30 in mutant M6. Furthermore, full-length recombinant HMW1 completely restored HMW2 in mutant M6 to a wild-type level (Fig. 2A and 3). Taken together with previous studies, which established that HMW2 is required for HMW1 stability (26), the present data demonstrate that HMW1 and HMW2 are in fact mutually stabilizing.

HMW2 fails to localize to the attachment organelle in the absence of HMW1. An HMW2-GFP fusion localizes to the attachment organelle and restores a largely wild-type phenotype to mutant I-2 (5). M6 transformants producing recombinant HMW2-GFP were examined here by phase-contrast–fluorescence microscopy to assess the impact of loss of HMW1 on HMW2 localization. Polar foci were observed in transformants

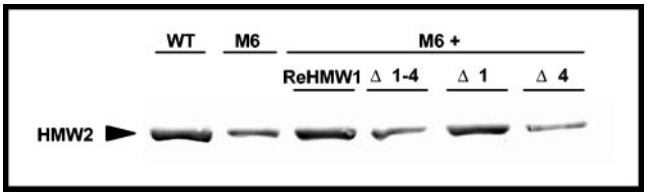

FIG. 3. Western immunoblot analysis of HMW2 steady-state levels in wild-type (WT) and mutant M6 *M. pneumoniae* and M6 producing the indicated HMW1 deletion derivatives (see Fig. 1). Mycoplasma samples were prepared as described above, with equal amounts of protein used for each sample. The arrowhead indicates HMW2.

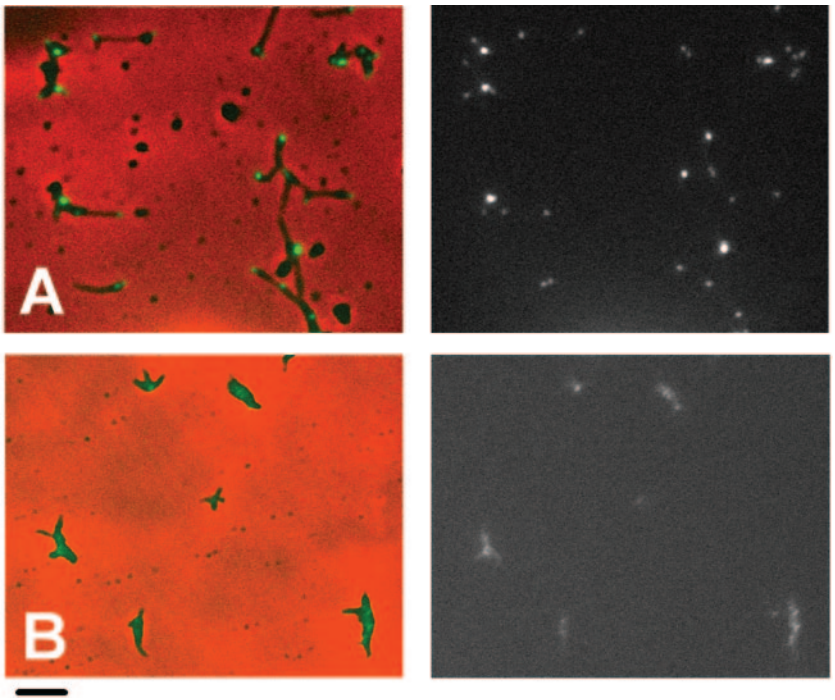

FIG. 4. Analysis of HMW2-GFP localization in *M. pneumoniae* mutants I-2 (A) and M6 (B). The left and right panels for each pair are images by merged phase-contrast and fluorescence microscopy, and fluorescence microscopy only, respectively. HMW2-GFP complements the *hmw2* gene defect in mutant I-2 (5). Bar, 2 μm.

of mutant I-2 producing HMW2-GFP (Fig. 4A), as expected (5). However, fluorescence intensity was both reduced and dispersed throughout the cells in M6 transformants producing HMW2-GFP, where faint clusters of fluorescence were also noted, although none specifically polar (Fig. 4B). In contrast, HMW2-GFP fluorescence in transformants of mutant II-7 was indistinguishable from that in wild-type or mutant I-2 *M. pneumoniae* (data not shown), indicating that failure of HMW2 to localize to the attachment organelle in mutant M6, like HMW2 instability, correlated specifically with loss of HMW1 and not truncation of P30. In all cases, multiple transformants were examined individually to control for possible consequences associated with the site of transposon insertion.

Deletion analysis of the HMW1 C-terminal region. Unlike its full-length counterpart, the truncated recombinant HMW1 derivative lacking the C-terminal 112 residues fails to restore near-normal cell morphology or the ability to localize P1 to the attachment organelle in mutant M6 (13). To define more precisely regions within the C-terminal domain of HMW1 essential for function, including HMW2 stabilization and localization, we engineered deletion derivatives based upon the location of a paired Ser motif repeated four times within this domain (Fig. 1A) and previously implicated as potentially important in targeting for accelerated turnover (26). Each was introduced into mutant M6 *M. pneumoniae* by transposon delivery, and multiple transformants were analyzed individually for stability and subcellular localization of the HMW1 derivative, P1 localization, stability and localization of HMW2, and cell morphology (Table 3).

Steady-state levels of full-length recombinant HMW1 and HMW1 Δ1 in mutant M6 were comparable to resident HMW1 in wild-type *M. pneumoniae*, while HMW1 Δ1–4 and HMW1 Δ4 were lower (Fig. 5); HMW1 Δ2–4, which lacks all but region 1 of the C-terminal domain (Fig. 1A), was extremely unstable (data not shown) and was not considered further here. Like resident HMW1 in wild-type *M. pneumoniae* (Fig. 6A), full-length recombinant HMW1 exhibited polar, focused fluorescence (Fig. 6E). HMW1 Δ1 likewise exhibited predominantly intense polar fluorescence, although cells with faint diffuse or no fluorescence were apparent (Fig. 6D). HMW1 Δ4, on the

TABLE 3. Phenotype summary of HMW1 deletion derivatives in *M. pneumoniae* mutant M6

HMW1 derivative	Stability	Localization	HMW2 stability[b]	P1 localization	Morphology
None	NA[a]	NA[a]	+	Diffuse	Coccoid; branching common
HMW1 Δ1-4	++	Diffuse; limited clustering	+	Diffuse	Coccoid; branching common
HMW1 Δ4	++	Mixed; polar or diffuse	+	Mixed; some polar	Elongated; branching common
HMW1 Δ1	++++	Intensely polar	+++	Mostly polar	Near-wild type
reHMW1	++++	Intensely polar	++++	Polar	Near-wild type

[a] NA, not applicable.
[b] Relative levels; ++++, wild type.

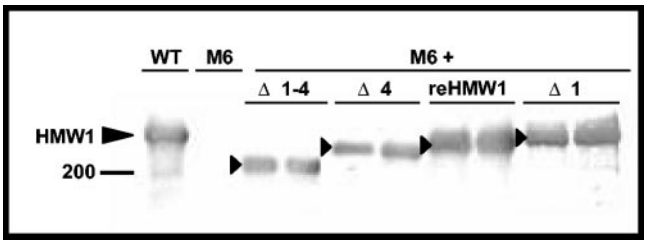

FIG. 5. Western immunoblot analysis of the stability of HMW1 deletion derivatives in mutant M6 *M. pneumoniae*. Two independent transformants are shown for each HMW1 derivative. Equal amounts of protein were loaded per lane, separated by electrophoresis, transferred to nitrocellulose, and probed with anti-HMW1 serum (1:10,000). WT, untransformed wild-type *M. pneumoniae*; M6, untransformed mutant M6; M6 +, M6 *M. pneumoniae* transformants producing the indicated HMW1 derivative. The large arrowhead indicates HMW1, while smaller arrowheads indicate recombinant HMW1 derivatives.

other hand (Fig. 6C), had much greater variation from polar to diffuse fluorescence and rendered M6 cells consistently less elongated and more branched than did full-length HMW1 or HMW1 Δ1, both of which restored a near-normal morphology. HMW1 Δ1–4 had little effect on cell morphology as expected (13) and exhibited diffuse, faint fluorescence with occasional discrete foci, indicating an apparent defect in localization (Fig. 6B).

The pattern for P1 localization largely paralleled that of the HMW1 derivatives. Polar fluorescence was observed for protein P1 in wild-type *M. pneumoniae* (Fig. 7A) but not M6 (Fig. 7B) or M6 producing HMW1 Δ1–4 (Fig. 7C), as expected (13). HMW1 Δ1 largely restored P1 localization (Fig. 7E), but an intermediate pattern of fluorescence was observed with HMW1 Δ4, where fluorescent foci were apparent but largely not polar (Fig. 7D).

Surprisingly, only full-length recombinant HMW1 fully restored HMW2 to wild-type levels in M6. HMW1 Δ1 partially restored HMW2, while HMW1 Δ1–4 and HMW1 Δ4 had no impact (Fig. 3), prompting the examination of HMW2 localization for each. Technical difficulties made the use of HMW2-GFP in M6 transformants producing recombinant HMW1 deletion derivatives impractical. Rather, we employed immunofluorescence microscopy with affinity-purified HMW2-specific antibodies and a modified blocking procedure to reduce background (see above). Fluorescence was faint but clearly consistent with localization results in Fig. 4 with HMW2-GFP, i.e., polar foci in wild-type *M. pneumoniae* and dispersed in otherwise untransformed mutant M6 (Fig. 8A and B, respectively). HMW2 likewise exhibited clustered polar fluorescence for HMW1 Δ1 (Fig. 8E) but not HMW1 Δ1–4 (Fig. 8C) and only rarely for HMW1 Δ4 (Fig. 8D). Thus, the C-terminal 41 residues deleted in HMW1 Δ4 were particularly important for HMW1 function in localization of HMW2 to the attachment organelle yet not sufficient to stabilize HMW2 fully.

DISCUSSION

Duplication of the attachment organelle is thought to be an early step in *M. pneumoniae* cell division, with a second terminal structure forming adjacent to the first and the two then localizing to opposite poles of the cell prior to cytokinesis (reviewed in reference 19). The electron-dense core of the attachment organelle is described as comprising twin flattened rods which appear to separate with attachment organelle duplication (15), raising the possibility of a semiconservative process whereby each rod serves as a template in attachment organelle development. Yet the ability of recombinant HMW1 or HMW2 to restore a functional attachment organelle in mutants lacking these proteins (10, 13) and for which no electron-dense core is apparent (31) suggests that de novo assembly may also be possible. It is likely in both cases that proper

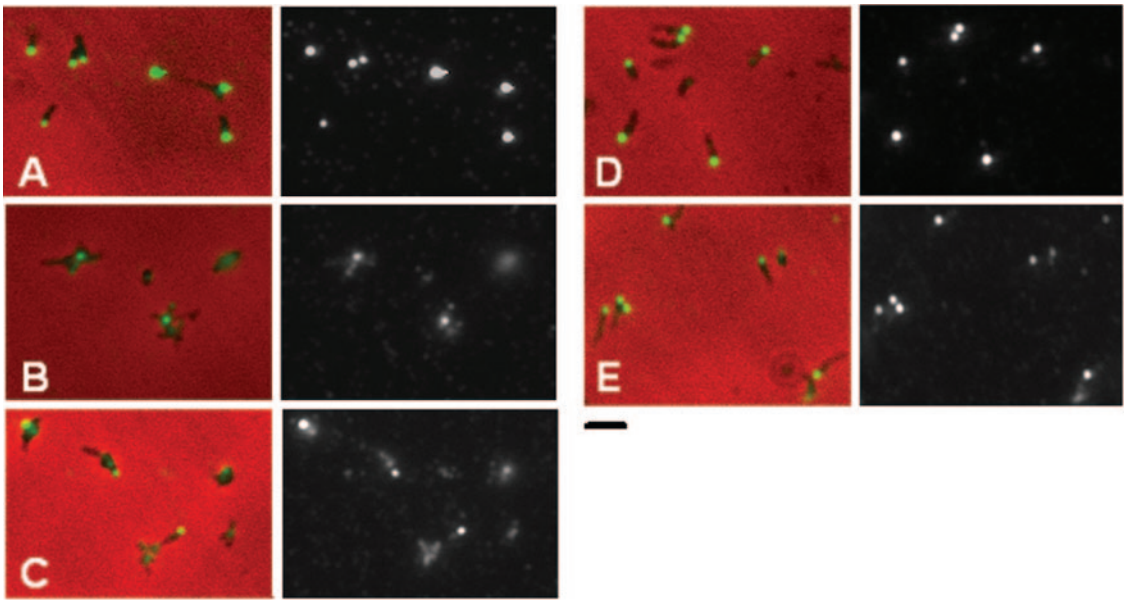

FIG. 6. Phase-contrast–immunofluorescence analysis of HMW1 localization in wild-type *M. pneumoniae* (A) and mutant M6 producing HMW1 Δ1–4 (B), HMW1 Δ4 (C), HMW1 Δ1 (D), or reHMW1 (E). For each pair, the merged immunofluorescence and phase-contrast images are shown on the left and the corresponding immunofluorescence images alone are shown on the right. Bar, 2.0 μm.

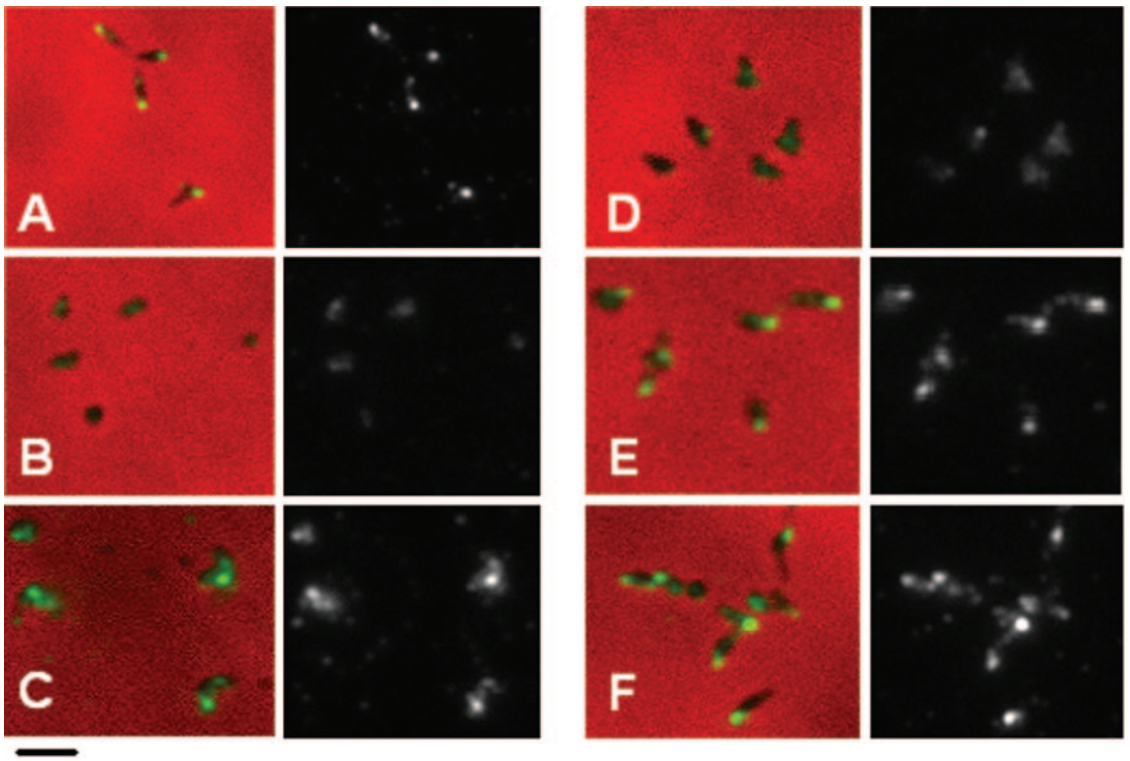

FIG. 7. Phase-contrast–immunofluorescence analysis of P1 localization in wild-type *M. pneumoniae* (A), mutant M6 (B), and mutant M6 producing HMW1 Δ1–4 (C), HMW1 Δ4 (D), HMW1 Δ1 (E), or reHMW1 (F). For each pair of images, the merged phase-contrast and immunofluorescence images are shown on the left, and the corresponding immunofluorescence images alone are shown on the right. Bar, 2.0 μm.

targeting and sequential assembly of component proteins is required to yield a fully functional structure (19). Furthermore, the mutual dependence of HMW1 and HMW2 for stability (this study), the requirement for each to form an electron-dense core (31), and the destabilizing effect of loss of either on other attachment organelle proteins are consistent with their joint involvement early in the assembly sequence (19).

The original description of mutant M6 reported only the loss of HMW1 due to a frameshift mutation and the truncation of P30 due to an in-frame deletion (22). Subsequent study of this strain revealed decreased levels of P65 as well (17). Continued characterization has now indicated that HMW2 levels are also reduced. The previous failure to detect a difference in steady-state HMW2 in mutant M6 can probably be attributed to difficulty resolving HMW2 by SDS-PAGE and staining, and problems generating satisfactory HMW2-specific antibodies (unpublished data); until the present study, the latter likewise plagued repeated attempts at immunolocalization and in a previous study prompted the use of a GFP fusion for this purpose (5). Nevertheless, reduced steady-state HMW2 in mutant M6 was readily apparent by Western immunoblotting (Fig. 2A); thus, HMW2 joins HMW1, HMW3, and P65 as components of the attachment organelle which are subject to accelerated turnover in certain mutant backgrounds (references 17 and 26 and this study).

Proteolytic turnover of unincorporated components of protein complexes is a common quality control measure for macromolecular assembly in a variety of bacteria. Examples include the proteins of the F_o subunit of ATPase (1, 16) and complexes of SecY, SecE, and SecG, which associate to form a channel through the inner membrane for protein secretion (18, 24, 34). Similar mechanisms for quality control occur with protein complexes from a variety of microorganisms (25, 27, 29), apparently including the mycoplasmas.

Newly synthesized HMW1 is thought to move from the cytoplasmic, TX-soluble fraction to a transiently TX-insoluble state and then to a stable, insoluble form on the cell surface in wild-type *M. pneumoniae* (2). This process occurs inefficiently in the absence of HMW2, shifting HMW1 equilibrium to the cytoplasmic fraction, where it is degraded (2, 26). Conversely, the present study demonstrates that HMW2 stability is dependent upon HMW1, while suggesting a dual role for HMW1 in attachment organelle assembly. First, HMW1 is required for localization of P1 to the attachment organelle, as demonstrated previously (13) and reinforced by the finding that recombinant deletion derivative HMW2 Δmid confers a near-wild-type phenotype to mutant I-2 but fails to stabilize and/or localize HMW1 or localize P1 (4). Likewise, P1 localization in the present study correlated with stabilization of HMW1 and localization of HMW1 to the attachment organelle. Taken together, these observations are consistent with a structural role for HMW1, perhaps associated in its extracellular state in a stable manner with the mycoplasma cytoskeleton. Second, full-length HMW1 is required, though not at wild-type levels (4), to stabilize HMW2 (this study); thus, reduced steady-state HMW1 was sufficient to stabilize HMW2 Δmid (4). Because HMW1 exists in both intracellular and extracellular states (2, 32) while HMW2 is thought to be strictly intracellular (5),

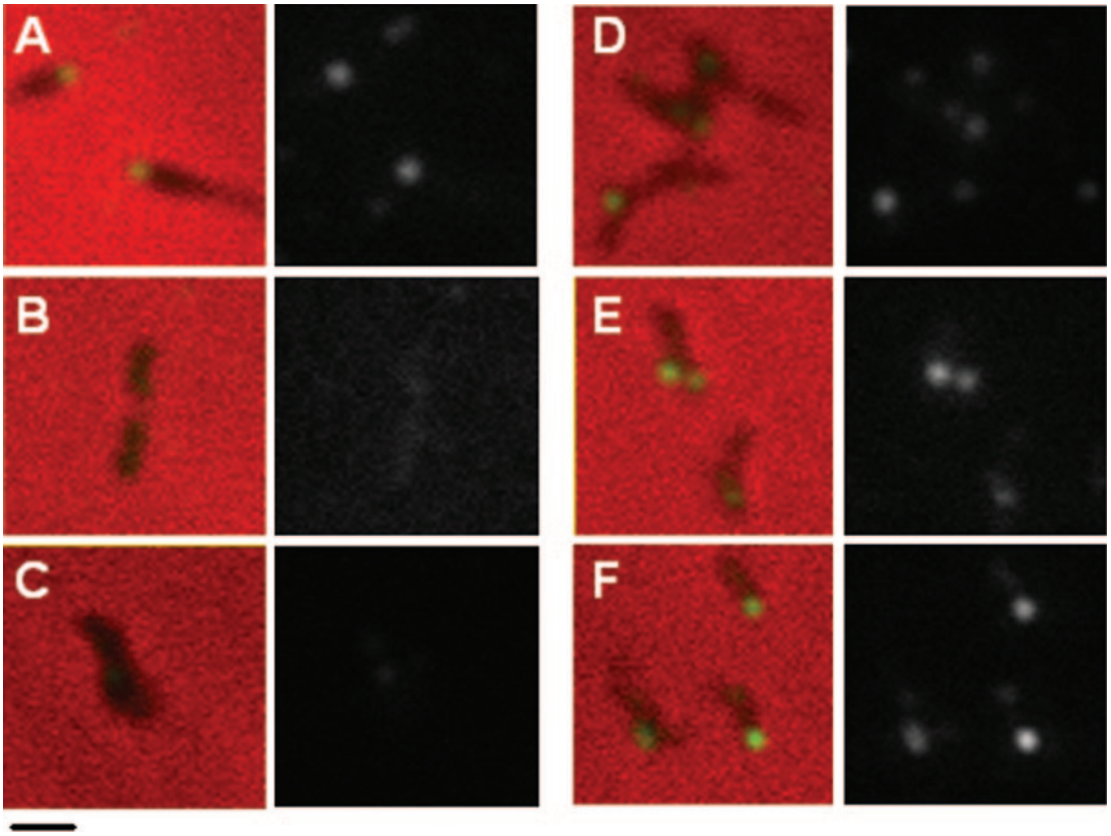

FIG. 8. Phase-contrast–immunofluorescence analysis of HMW2 localization in wild-type *M. pneumoniae* (A), mutant M6 (B), and M6 transformants producing HMW1 Δ1–4 (C), HMW1 Δ4 (D), HMW1 Δ1 (E), or reHMW1 (F). For each pair of images, the merged phase-contrast and immunofluorescence images are shown on the left and the corresponding immunofluorescence images alone are shown on the right. Bar, 1.0 μm.

potential direct interaction would apparently be limited to the intracellular HMW1 pool. Alternatively, indirect interaction could occur with extracellular HMW1 through one or more additional proteins. Regardless, stoichiometry does not appear to be a factor in the requirement for HMW1 to stabilize and/or localize HMW2, where, for example, newly synthesized, cytoplasmic HMW1 might act catalytically in a manner analogous to chaperones before its stable association with the cytoskeleton and export to the cell surface.

The C-terminal domain of HMW1 is required for proper localization to the attachment organelle (this study), for normal function in cell morphology (13), for its accelerated turnover in the absence of HMW2 (26), and to stabilize HMW2 (this study). HMW1 Δ1 fully restored HMW2 localization to the attachment organelle in mutant M6 and partially restored HMW2 stability. However, HMW1 Δ4 did not restore HMW2 stability, exhibited a poor capacity to localize properly, and yielded highly variable localization of P1 and HMW2 and cell morphology. Thus, while a fully intact HMW1 C-terminal domain is required to stabilize HMW2 at wild-type levels, the C-terminal 41 residues of HMW1 are particularly important for localization of HMW2 to the attachment organelle at wild-type efficiency. Significantly, preliminary data indicate that formation of the electron-dense core in these transformants exhibits a similar pattern, with core formation correlating with HMW2 stability (unpublished data).

The present study demonstrates a reciprocal dependency between HMW1 and HMW2, indicates a requirement for HMW1 in localization of HMW2 to the attachment organelle, identifies the C-terminal 41 residues of HMW1 as having functional significance, and raises questions about the nature and timing of a potential interaction between HMW1 and HMW2 in attachment organelle biogenesis. As more information emerges regarding the identity of functional domains of each protein, it should be feasible to explore HMW1-HMW2 interactions more directly.

ACKNOWLEDGMENTS

This work was supported in part by Public Health Service Research Grant AI22362 from the National Institute of Allergy and Infectious Diseases to D.C.K., by training support awarded to M.J.W. from a National Science Foundation Research Training Grant in Prokaryotic Diversity (NSF BIR9413235), and by Public Health Service National Research Service Award AI10500 to M.F.B.

REFERENCES

1. **Akiyama, Y., A. Kihara, and K. Ito.** 1996. Subunit a of proton ATPase F0 sector is a substrate of the FtsH protease in *Escherichia coli.* FEBS Lett. **399:**26–28.
2. **Balish, M. F., T. W. Hahn, P. L. Popham, and D. C. Krause.** 2001. Stability of *Mycoplasma pneumoniae* cytadherence-accessory protein HMW1 correlates with its association with the triton shell. J. Bacteriol. **183:**3680–3688.
3. **Balish, M. F., and D. C. Krause.** 2002. Cytadherence and the cytoskeleton, p. 491–518. *In* S. Razin and R. Herrmann (ed.), Molecular biology and pathogenicity of the mycoplasmas. Kluwer Academic/Plenum Publishers, New York, N.Y.

4. **Balish, M. F., S. M. Ross, M. Fisseha, and D. C. Krause.** 2003. Deletion analysis identifies key functional domains of the cytadherence-associated protein HMW2 of *Mycoplasma pneumoniae*. Mol. Microbiol. **50:**1507–1516.
5. **Balish, M. F., R. T. Santurri, A. M. Ricci, K. K. Lee, and D. C. Krause.** 2003. Localization of *Mycoplasma pneumoniae* cytadherence-associated protein HMW2 by fusion with green fluorescent protein: implications for attachment organelle structure. Mol. Microbiol. **47:**49–60.
6. **Baseman, J. B., R. M. Cole, D. C. Krause, and D. K. Leith.** 1982. Molecular basis for cytadsorption of *Mycoplasma pneumoniae*. J. Bacteriol. **151:**1514–1522.
7. **Biberfeld, G., and P. Biberfeld.** 1970. Ultrastructural features of *Mycoplasma pneumoniae*. J. Bacteriol. **102:**855–861.
8. **Dallo, S. F., A. L. Lazell, A. Chavoya, S. P. Reddy, and J. B. Baseman.** 1996. Biofunctional domains of the *Mycoplasma pneumoniae* P30 adhesin. Infect. Immun. **64:**2595–2601.
9. **Dirksen, L. B., T. Proft, H. Hilbert, H. Plagens, R. Herrmann, and D. C. Krause.** 1996. Sequence analysis and characterization of the *hmw* gene cluster of *Mycoplasma pneumoniae*. Gene **171:**19–25.
10. **Fisseha, M., H. W. Göhlmann, R. Herrmann, and D. C. Krause.** 1999. Identification and complementation of frameshift mutations associated with loss of cytadherence in *Mycoplasma pneumoniae*. J. Bacteriol. **181:**4404–4410.
11. **Göbel, U., V. Speth, and W. Bredt.** 1981. Filamentous structures in adherent *Mycoplasma pneumoniae* cells treated with nonionic detergents. J. Cell Biol. **91:**537–543.
12. **Hahn, T.-W., K. A. Krebes, and D. C. Krause.** 1996. Expression in *Mycoplasma pneumoniae* of the recombinant gene encoding the cytadherence-associated protein HMW1 and identification of HMW4 as a product. Mol. Microbiol. **19:**1085–1093.
13. **Hahn, T.-W., M. J. Willby, and D. C. Krause.** 1998. HMW1 is required for cytadhesin P1 trafficking to the attachment organelle in *Mycoplasma pneumoniae*. J. Bacteriol. **180:**1270–1276.
14. **Hedreyda, C. T., K. K. Lee, and D. C. Krause.** 1993. Transformation of *Mycoplasma pneumoniae* with Tn*4001* by electroporation. Plasmid **30:**170–175.
15. **Hegermann, J., R. Herrmann, and F. Meyer.** 2002. Cytoskeletal elements in the bacterium *Mycoplasma pneumoniae*. Naturwissenschaften. **89:**453–458.
16. **Hermolin, J., and R. H. Fillingame.** 1995. Assembly of F_0 sector of *Escherichia coli* H+ ATP synthase. Interdependence of subunit insertion into the membrane. J. Biol. Chem. **270:**2815–2817.
17. **Jordan, J. L., K. M. Berry, M. F. Balish, and D. C. Krause.** 2001. Stability and subcellular localization of cytadherence-associated protein P65 in *Mycoplasma pneumoniae*. J. Bacteriol. **183:**7387–7391.
18. **Kihara, A., Y. Akiyama, and K. Ito.** 1995. FtsH is required for proteolytic elimination of uncomplexed forms of SecY, an essential protein translocase subunit. Proc. Natl. Acad. Sci. USA **92:**4532–4536.
19. **Krause, D. C., and M. F. Balish.** 2004. Cellular engineering in a minimal microbe: structure and assembly of the terminal organelle of *Mycoplasma pneumoniae*. Mol. Microbiol. **51:**917–924.
20. **Krause, D. C., D. K. Leith, R. M. Wilson, and J. B. Baseman.** 1982. Identification of *Mycoplasma pneumoniae* proteins associated with hemadsorption and virulence. Infect. Immun. **35:**809–817.
21. **Krause, D. C., T. Proft, C. T. Hedreyda, H. Hilbert, H. Plagens, and R. Herrmann.** 1997. Transposon mutagenesis reinforces the correlation between *Mycoplasma pneumoniae* cytoskeletal protein HMW2 and cytadherence. J. Bacteriol. **179:**2668–2677.
22. **Layh-Schmitt, G., H. Hilbert, and E. Pirkl.** 1995. A spontaneous hemadsorption-negative mutant of *Mycoplasma pneumoniae* exhibits a truncated adhesin-related 30-kilodalton protein and lacks the cytadherence-accessory protein HMW1. J. Bacteriol. **177:**843–846.
23. **Lipman, R. P., W. A. Clyde, Jr., and F. W. Denny.** 1969. Characteristics of virulent, attenuated, and avirulent *Mycoplasma pneumoniae* strains. J. Bacteriol. **100:**1037–1043.
24. **Matsuyama, S., J. Akimaru, and S. Mizushima.** 1990. SecE-dependent overproduction of SecY in *Escherichia coli*. Evidence for interaction between two components of the secretory machinery. FEBS Lett. **269:**96–100.
25. **Michel, G., S. Bleves, G. Ball, A. Lazdunski, and A. Filloux.** 1998. Mutual stabilization of the XcpZ and XcpY components of the secretory apparatus in *Pseudomonas aeruginosa*. Microbiology **144:**3379–3386.
26. **Popham, P. L., T.-W. Hahn, K. A. Krebes, and D. C. Krause.** 1997. Loss of HMW1 and HMW3 in noncytadhering mutants of *Mycoplasma pneumoniae* occurs post-translationally. Proc. Natl. Acad. Sci. USA **94:**13979–13984.
27. **Possot, O. M., G. Vignon, N. Bomchil, F. Ebel, and A. P. Pugsley.** 2000. Multiple interactions between pullulanase secreton components involved in stabilization and cytoplasmic membrane association of PulE. J. Bacteriol. **182:**2142–2152.
28. **Sambrook, J., E. F. Fritsch, and T. Maniatis.** 1989. Molecular cloning: a laboratory manual, 2nd ed. Cold Spring Harbor Laboratory Press, Cold Spring Harbor, N.Y.
29. **Sandkvist, M., M. Bagdasarian, S. P. Howard, and V. J. DiRita.** 1995. Interaction between the autokinase EpsE and EpsL in the cytoplasmic membrane is required for extracellular secretion in *Vibrio cholerae*. EMBO J. **14:**1664–1673.
30. **Seto, S., G. Layh-Schmitt, T. Kenri, and M. Miyata.** 2001. Visualization of the attachment organelle and cytadherence proteins of *Mycoplasma pneumoniae* by immunofluorescence microscopy. J. Bacteriol. **183:**1621–1630.
31. **Seto, S., and M. Miyata.** 2003. Attachment organelle formation represented by localization of cytadherence proteins and formation of the electron-dense core in wild-type and mutant strains of *Mycoplasma pneumoniae*. J. Bacteriol. **185:**1082–1091.
32. **Stevens, M. K., and D. C. Krause.** 1991. Localization of the *Mycoplasma pneumoniae* cytadherence-accessory proteins HMW1 and HMW4 in the cytoskeletonlike Triton shell. J. Bacteriol. **173:**1041–1050.
33. **Stevens, M. K., and D. C. Krause.** 1992. *Mycoplasma pneumoniae* cytadherence phase-variable protein HMW3 is a component of the attachment organelle. J. Bacteriol. **174:**4265–4274.
34. **Taura, T., T. Baba, Y. Akiyama, and K. Ito.** 1993. Determinants of the quantity of the stable SecY complex in the *Escherichia coli* cell. J. Bacteriol. **175:**7771–7775.
35. **Tully, J. G., R. F. Whitcomb, H. F. Clark, and D. L. Williamson.** 1977. Pathogenic mycoplasmas: cultivation and vertebrate pathogenicity of a new spiroplasma. Science **195:**892–894.
36. **Willby, M. J., and D. C. Krause.** 2002. Characterization of a *Mycoplasma pneumoniae hmw3* mutant: implications for attachment organelle assembly. J. Bacteriol. **184:**3061–3068.